Supplementary Information

Tailoring zirconium-based MOF architectures for uptaking targeted micropollutants with high risk: The critical role of porphyrin ligands in adsorption-catalysis processes

Tiantian Zhu[1, #], Qiao Jiang[1,2,#], Yuxin Lu[1, #],Yazi Meng[1], Yuhua Cao[1], Ke Li[3], Bo Wang (✉)[1], Xiang Li (✉)[1]

1 School of Chemistry and Chemical Engineering, Key Laboratory of Cluster Science, Ministry of Education, Beijing Key Laboratory of Photoelectronic/Electrophotonic Conversion Materials, Advanced Technologies Research Institute (Jinan), Advanced Research Institute of Multidisciplinary Science, Beijing 100081, China

2 Department of Chemistry, School of Science, Institute of Science Tokyo, Tokyo 152-8550, Japan

3 College of Engineering, University of Georgia, Athens GA 30602, USA

Table S1 Experimental reagents.

Reagents	Manufacturer	**Origin**	Purity
$ZrCl_4$	Energy Chemical	China	98%
$ZrOCl_2\cdot 8H_2O$	Energy Chemical	China	99%
H_2BDC	Energy Chemical	China	99%
$H_2BDC-NH_2$	Aladdin Scientific	China	≥98.0%
H_2TCPP	Yuanye Bio Tech	China	≥97%
TFA	Energy Chemical	China	99%
2FBA	Aladdin Scientific	China	≥98.0%
HCl	Tianjin Fine Chemicals	China	AR
HCOOH	Energy Chemical	China	HPLC
NaOH	Aladdin Scientific	China	99.0%
CH_3COONH_4	Aladdin Scientific	China	99.0%
H_2O	Watsons	China	Distilled water
CH_3OH	Sinopharm	China	AR
CH_3OH	Energy Chemical	China	HPLC/ACS
DMF	Sinopharm	China	AR
C_2H_5OH	Sinopharm	China	AR
BPA	HEOWNS	China	99%
NPX	Yuanye Bio Tech	China	≥98%
NFX	Yuanye Bio Tech	China	≥98%
TC	Yuanye Bio Tech	China	≥95%
PBQ	Aladdin Scientific	China	99%

✉ Corresponding authors

E-mail: bowang@bit.edu.cn (B. Wang); lixiang@bit.edu.cn (X. Li)

Tiantian Zhu[1, #], Qiao Jiang[1,2,#], and Yuxin Lu[1, #], the authors contributed equally to this work and should be considered co-first authors.

Table S2 Glossary of terms and abbreviations.

Term	Definition
BPA	Bisphenol A
DMF	Dimethylformamide
DMPO	5,5-dimethyl-1-pyrroline N-oxide
HPLC	High performance liquid chromatography
EOCs	Emerging organic contaminants
ESR	Electron spin resonance
FTIR	Fourier transform infrared spectroscopy
H_2BDC	Terephthalic acid
H_2BDC-NH	Dimethyl amino terephthalate
H_2TCPP	Meso-Tetra (4-carboxyphenyl) porphyrin
LCCT	Ligand-cluster charge transfer
MOFs	Metal-organic frameworks
NFX	Norfloxacin
NPX	Naproxen
NSAIDs	Nonsteroidal anti-inflammatory drugs
PBQ	p-Benzoquinone
PPCPs	Pharmaceuticals and personal care products
PXRD	Powder X-ray diffraction
ROS	Reactive oxygen species
SEM	Scanning electron microscope
TC	Tetracycline
TFA	Trifluoroacetic acid
WWTPs	Wastewater treatment plants
2FBA	2-fluorobenzoic acid

Table S3 Experimental equipment.

Sample Characterization	Equipment	Origin	Type
Sample surface morphology	JSM-IT200 Schottky field-emission scanning electron microscope (SEM)	ZEISS (Germany)	SUPRA S5
Powder X-ray diffraction (PXRD) patterns	Rigaku MiniFlex600 diffractometer (Cu-Kα X-ray source, λ = 0.154056 nm)	Rigaku (Japan)	MiniFlex 600
Nitrogen adsorption-desorption isotherms	Bruker D8 Advance automated volumetric gas sorption analyzer	BEIJING BUILDER ELECTRONIC TECHNOLOGY CO.,LTD (China)	SSA-4200
Microwave reactor	NOVA-2S single-mode microwave	Preekem	NOVA-2S

	synthesis system	(China)	
Fourier-transform infrared (FTIR) spectra	Bruker ALPHA FTIR spectrometer	Thermo scientific (USA)	NiColet is50 FT-IR
Concentration analysis of PPCPs in liquid samples	Shimadzu LC-20A high-performance liquid chromatography (HPLC) system, Agilent HPLC column (ZORBAX SB-C18, 4.6 × 150 mm, 5 μm particle size)	Agilent (USA)	1260 II
Zeta potential in aqueous systems	Malvern Zetasizer Nano ZS90	Malvern (UK)	Nano-ZS ZEN3600
Light source for photocatalytic experiments	CEL-PE300L-3A xenon lamp light source (Beijing China Education Au-Light Co., Ltd.)	Beijing China Education Au-light Co., Ltd (China)	CEL-PE300L-3A
Light power density measurement	Thorlabs PM100D optical power meter	Beijing China Education Au-light Co., Ltd (China)	PM100D
Electron spin resonance (ESR) spectra	Bruker EMXplus A300 ESR spectrometer	Bruker (Germany)	EMX plus

Table S4 Summary of photocatalytic performance of NH_2-UiO-66 and PCN-222.

PPCPs	Parameter	NH_2-UiO-66	PCN-222
BPA	k / min	-	0.0318
	q_e / mg/g	-	59.8
	R^2	-	0.977
	20-h adsorption efficiency	4.15 %	60.9%
	2-h degradation efficiency	-	33.2%
NFX	k / min	-	0.0124
	q_e / mg/g	-	84.2
	R^2	-	0.958
	20-h adsorption efficiency	25.4 %	67.7%
	2-h degradation efficiency	-	15.8%
NPX	k / min	-	0.0101
	q_e / mg/g	-	135.1
	R^2	-	0.991
	20-h adsorption efficiency	3.67 %	31.7%
	2-h degradation efficiency	-	36.6%

TC	k / min	0.0150	0.631
	q_e / mg/g	162	75.0
	R^2	0.972	0.992
	20-h adsorption efficiency	11.1 %	79.6%
	2-h degradation efficiency	33.4 %	16.3%

Table S5 The properties and structure of pollutants.

Pollutants	Charge	Weight	Structure
Ketoprofen （KP）	negative	257.3	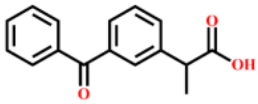
Antipyrine （AT）	positive	189.1	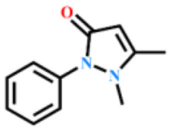
Ibuprofen （IBU）	negative	205.1	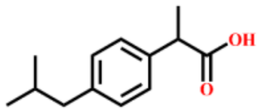
Chloramphenicol （CAP）	positive	321.0	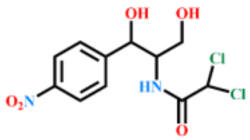
Sulfamethoxazole （SMX）	positive	254.1	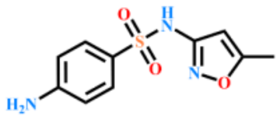
Sulfachloropyrazine sodium （SSM）	positive	284.7	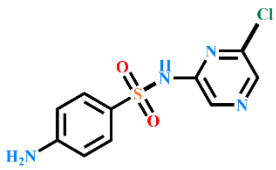
Indomethacin （IM）	negative	357.8	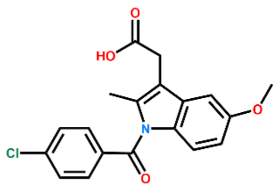
Clofibric acid （CA）	negative	214.7	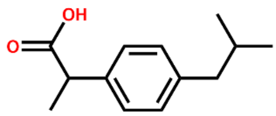

Table S6 The performance of SSM degradation by the reported work.

Photocatalysts	Condition	Removal rate	Degradation time	Refs.

2.0 g/L PDMAA–TiO_2/CuS	50 mL 25 mg/L	93.51%	16 h	(Guo et al., 2022)
2.5 g/L TiO_2	25 mL 25 mg/L	94%	60 min	(Ismail et al., 2016)
2.5 g/L UV/TiO_2/$K_2S_2O_8$	25 mL 88 μmol/L	100%	40 min	(Ismail et al., 2017)
0.04 g/L PCN-222	50 mL 1000 μg/L	99%	10 min	This work

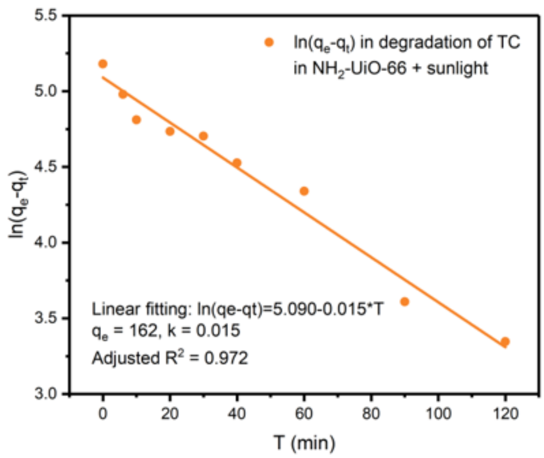

Fig. S1 The pseudo-first-order kinetic fitting plot for the catalytic degradation of TC by NH_2-UiO-66.

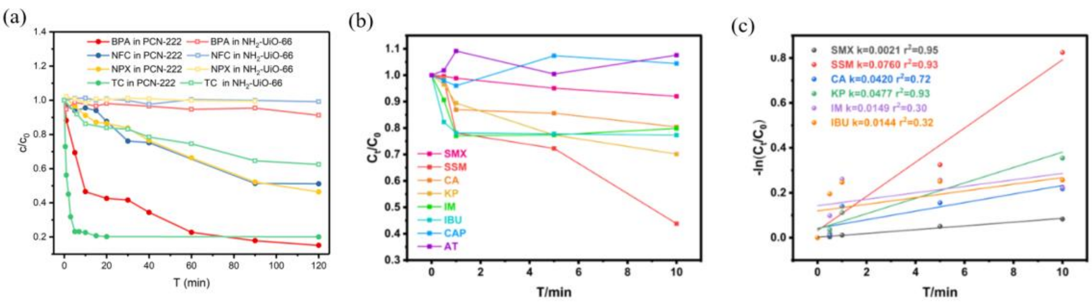

Fig. S2 (a) Comparative catalytic degradation efficiency of NH_2-UiO-66 and PCN-222 for four PPCPs. (b) Photocatalytic degradation of PCN-222 to mixed solutions of various PPCPs at environmental concentrations; (c) Photocatalytic degradation kinetics (experimental conditions: adsorbent dosage = 2 mg, reaction volume = 50 mL, reaction time = 10 min, initial concentration = 400 μg/L, filter: AM 1.5).

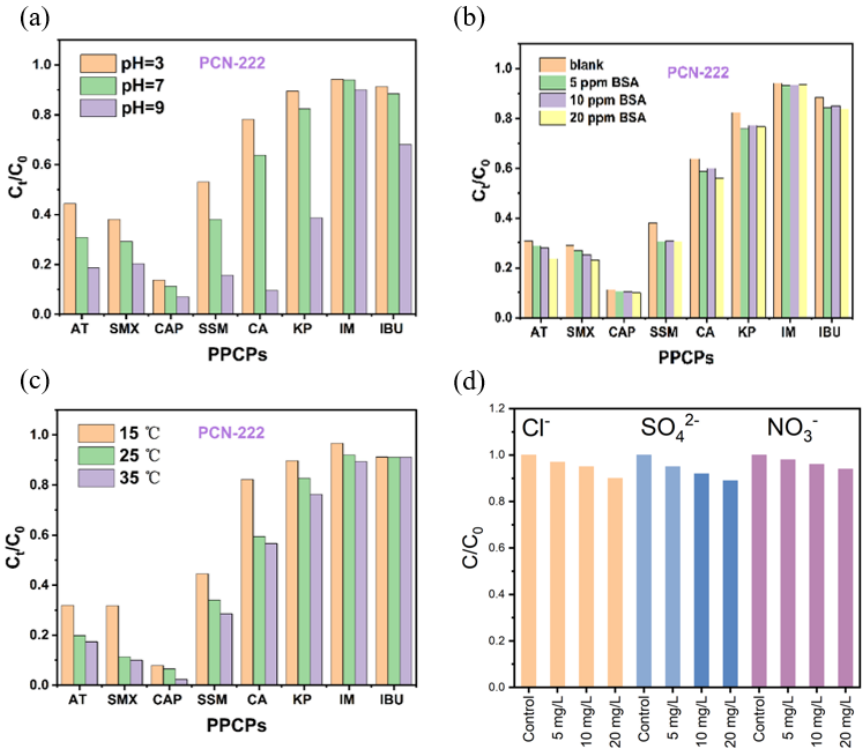

Fig. S3 Adsorption removal rate of PCN-222 for various substances at (a) different pH levels, (b) different temperatures, (c) with 5–20 ppm BSA, (d) under different ionic environments (experimental conditions: adsorbent dosage = 2 mg, reaction volume = 50 mL, reaction time = 120 min, initial concentration = 200 μg/L).

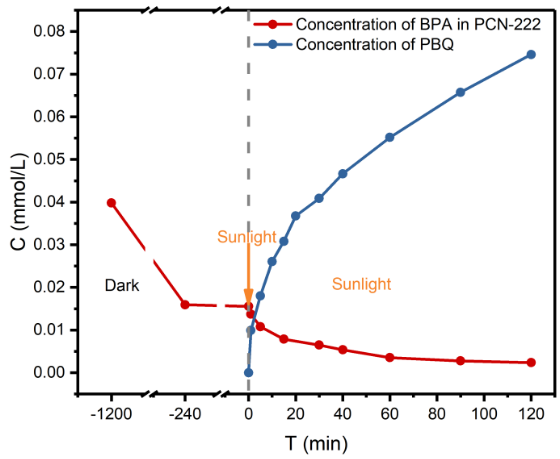

Fig. S4 Concentration profiles of BPA degradation and PBQ Formation by PCN-222.

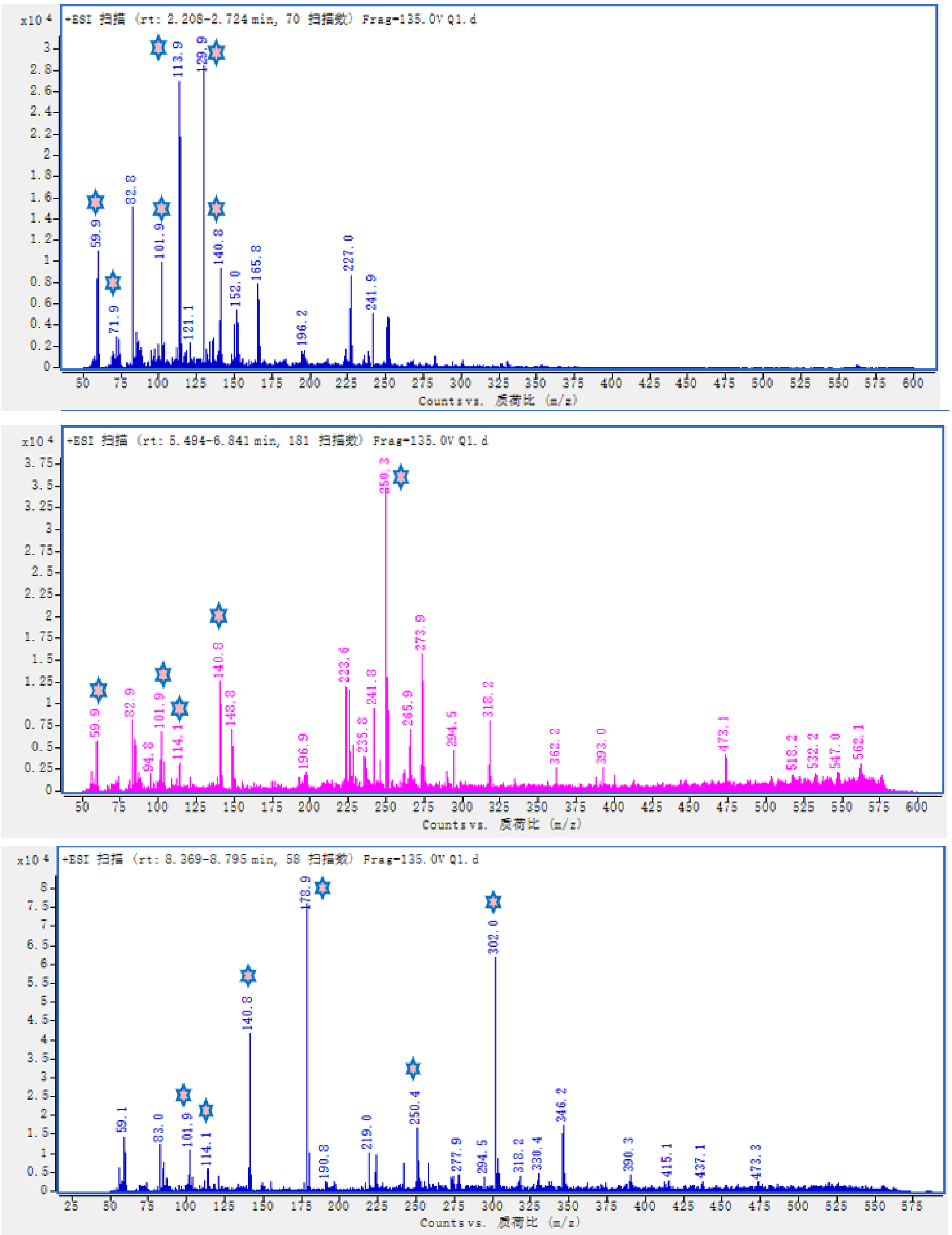

Fig. S5 The HPLC-MS/MS spectrum of intermediates during SSM degradation by PCN-222.

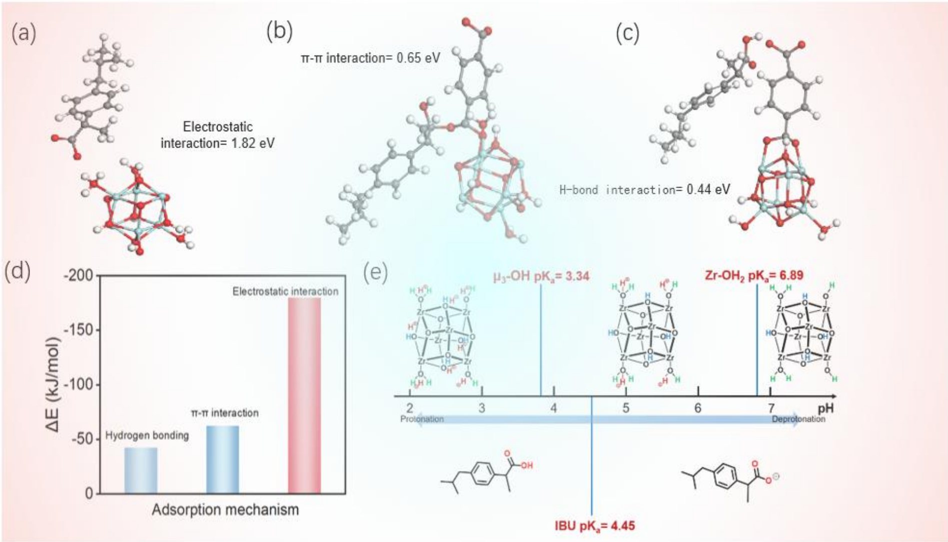

Fig. S6 The adsorption mechanism of (a) electrostatic interaction, (b) π-π interaction, and (c) H-bond interaction. (d) The adsorption energy of three mechanisms. (e) The chemical structure of pharmaceuticals under different pH values.